

Chapter 12

ULTRASHORT LASERS AND THEIR BIOEFFECTS

BENJAMIN A. ROCKWELL, PhD,* AND WILLIAM P. ROACH, PhD†

INTRODUCTION

WHAT MAKES ULTRASHORT LASER PULSES DIFFERENT?

- Spectral Content of Laser Pulse
- Peak Power
- Generation With Chirped Pulse Amplification

MEASUREMENT OF ULTRASHORT LASER PULSES

- Traditional Measurement Techniques
- Interferometric Measurements: Autocorrelation

ULTRASHORT LASER EFFECTS ON THE RETINA

- Nanosecond to Femtosecond Minimum Visible Lesion Thresholds
- Damage Mechanisms

ULTRASHORT LASER EFFECTS ON THE SKIN

ULTRAFAST, ULTRAINTENSE LASERS

SUMMARY

*Principal Research Physicist, Air Force Research Laboratory, 711th Human Performance Wing, Human Effectiveness Directorate, Bioeffects Division, Optical Radiation Bioeffects Branch, 4141 Petroleum Road, Joint Base San Antonio, Fort Sam Houston, Texas 78234-2644

†Chief, Physical and Biological Sciences Branch, Air Force Research Laboratory, Air Force Office of Scientific Research, 875 North Randolph Street, Arlington, Virginia 22203-1768

INTRODUCTION

Previous chapters in this volume present basic information related to the biomedical implications of military lasers. Traditional laser applications involve possible exposures to laser light with pulse durations ranging from as long as several seconds of continuous exposure to as short as several billionths of a second. Novel applications are emerging for lasers with much shorter pulse durations within the “ultrashort regime,” pulses with duration in the range of trillionths to quadrillionths of a second. (This chapter refers to quadrillion in the American English context, that is, the number 1 divided by 1 followed by 15 zeros.)

The traditional terminology of *ultrashort lasers* uses scientific notation to describe the pulse duration in seconds. One such term is *femtosecond* (also abbreviated as “fs”), which is equal to one-quadrillionth (1/1,000,000,000,000,000) of a second, expressed in scientific notation as 1×10^{-15} s. In Britain and in Germany, quadrillion refers to the number 1 followed by 24 zeros. In the British vernacular, the number 1 followed by 15 zeros is referred to as one septillion. Another relevant term is *picosecond* (also abbreviated as “ps”), which is one-trillionth (1/1,000,000,000,000) of a second, expressed in scientific notation as 1×10^{-12} s. Ultrashort pulses generally have durations between 10 fs and 500 ps. In this regime, novel phenomena occur that produce never-before-possible results. Several basic properties of ultrashort laser pulse systems set them apart from longer pulse systems. This chapter consid-

ers the most relevant differences related to laser–tissue interaction—which includes spectral content of the pulse, peak power, and the special techniques—that are required to produce and measure ultrashort pulses.

The field of *ultrashort-pulse laser technology* is now an established field, and femtosecond lasers offer revolutionary solutions to many of today’s toughest problems. Associated novel nonlinear optical phenomena support multiphoton biomedical imaging and treatment^{1–3} and precise alteration of cells.^{4–6} Femtosecond lasers have also been used to alter the refractive index of glass at a depth to inscribe light pipes.^{7,8} Some spectroscopic techniques may benefit from the application of ultrashort laser pulse technology, the unique attributes of which include their ability to generate coherent white light.⁹

Military applications are not yet in use, but the introduction of military ultrashort laser systems is inevitable. The current military arsenal includes laser systems that are continuous wave (CW) or pulsed, some of which could be adapted to the use of femtosecond laser technology. Because the spatial extent of an ultrashort laser is several microns, application of this technology could be used to support high-precision laser ranging and LIDAR (LIght Detection And Ranging). Ultrashort lasers have already been applied in science and medicine, and will eventually be used by the military. Therefore, it is essential that ultrashort laser–tissue interaction effects be understood.

WHAT MAKES ULTRASHORT LASER PULSES DIFFERENT?

Spectral Content of Laser Pulse

Sunlight dispersed through a prism (or dispersed in the form of a rainbow) provides an example of how a beam of light can be made up of a broad spectrum of light. In fact, sunlight includes components of much of the ultraviolet, visible, and infrared ranges of the electromagnetic spectrum. Some portions of the spectrum are absorbed by the Earth’s atmosphere, but most of the visible and near-infrared components reach the Earth’s surface. The sun’s spectral output is very large. The extent of its output is expressed in terms of the *bandwidth* of the spectral emission and its spread in wavelength ($\Delta\lambda$). The sun’s spectral bandwidth is hundreds of nanometers ($1 \text{ nm} = 0.001 \mu\text{m} = 10^{-9} \text{ m}$).

In contrast to the sun, traditional laser output is typically characterized by a very well-defined wavelength bandwidth less than 1/10 of 1 nm. Put through a prism, an ordinary laser beam (eg, HeNe [helium-neon] or

laser diode) would produce no discernable wavelength spread. Although some lasers can simultaneously produce output at several distinct wavelengths, each laser line itself has a very narrow bandwidth. An exception to this is the ultrashort laser.

A fundamental law of quantum physics known as the “uncertainty principle” asserts that as pulse duration is decreased, bandwidth must increase. This is not an easily measurable effect until pulse durations decrease well below 50 ps. For laser pulses below 50 fs, this property dramatically affects every aspect of pulse propagation, even through air. To capture the relative values of the bandwidth for ultrashort pulses, one must evaluate the following relationship between minimum pulse duration and minimum wavelength bandwidth:

$$\Delta\tau_{FWHM}\Delta\lambda_{FWHM} = \frac{2 \cdot \lambda^2}{\pi \cdot c} \ln 2 = \frac{0.4413}{c} \lambda^2,$$

where

$\Delta\tau_{FWHM}$ = pulse width,
 $\Delta\lambda_{FWHM}$ = bandwidth,
 c = speed of light, and
 λ = center wavelength.

Table 12-1 lists a range of minimum bandwidths required for femtosecond pulses as a function of pulse width and wavelength.

As can be seen in Table 12-1, wavelength bandwidths for pulses in the shorter femtosecond regime are significant, much different than traditional laser output. There are several consequences of this spectral content. First, generation of femtosecond pulses cannot be done using traditional lasing materials such as Nd:YAG (neodymium-doped yttrium aluminum garnet), which supports output wavelength on the order of nanometers and thus cannot be used to generate pulses shorter than a few picoseconds. Second, the broad bandwidth of the ultrashort laser affects propagation. Every optical material has a refractive index, which is dependent on wavelength. For example, water has a refractive index¹⁰ of 1.337 at 500 nm and 1.328 at 1,000 nm. This means that the longer wavelength portion of a femtosecond pulse travels through water at a higher speed than the shorter wavelength portion. Because of this, the pulse lengthens as it travels through water. The term for this effect is *group velocity dispersion (GVD)*. The extent of GVD for a given distance will depend directly on the refractive index and how it changes with wavelength. Therefore, even the simple propagation of femtosecond pulses can be a complex phenomenon.

Peak Power

For a given pulse energy, peak power is directly related to pulse duration. For example, a 10 ns pulse with a pulse energy of 100 mJ has a peak power of 10 MW. If this same pulse energy is applied as a 1 ps pulse, its peak power is 100 GW (1 GW = 1×10^9 W) or one-tenth of a *terawatt* (1 TW = 1×10^{12} W). At peak powers of even a few gigawatts, significant nonlinear optical processes can occur in either propagation or interaction. For example, if a 1 mJ pulse is focused with a pulse duration of 10 ns into a square block of glass, a laser-induced breakdown (LIB) occurs and the material is permanently damaged. If the same pulse is delivered at a pulse duration of 50 fs, it can produce a broad spectrum of light known as a *supercontinuum*.¹¹

Generation With Chirped Pulse Amplification

Materials have been created to support lasing action across a broad bandwidth range. The most common material used today is a sapphire crystal doped with a small percentage of titanium, known as Ti:Sapph

TABLE 12-1
MINIMUM BANDWIDTH IN NANOMETERS
OF ULTRASHORT LASER PULSE REQUIRED
TO GENERATE A PULSE OF THE GIVEN
DURATION

Pulse Duration (fs)	Center Wavelength			
	450 nm	800 nm	1,060 nm	1,300 nm
10,000 (10 ps)	0.03	0.009	0.17	0.25
1,000 (1 ps)	0.3	0.9	1.7	2.5
100	3.0	9.4	17	25
50	6.0	19	33	50
20	15	47	83	124
10	30	94	165	249

(titanium-sapphire). Figure 12-1 illustrates typical optical schematics for a femtosecond oscillator (*top*) and a femtosecond amplifier (*bottom*). The distinction between these two types of systems is important to consider for applications and the possibility of tissue effects.

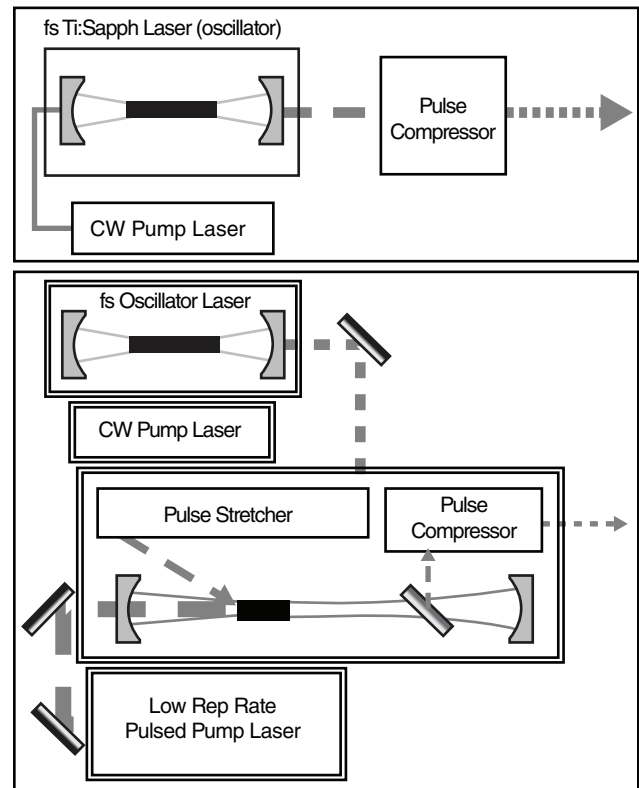


Figure 12-1. The typical setup for a femtosecond laser oscillator (*top*) and femtosecond amplifier (*bottom*). CW: continuous wave; fs: femtosecond; Rep: repetition; Ti:Sapph: titanium-sapphire

There are several differences between the femtosecond oscillator and the femtosecond amplifier. The femtosecond oscillator generates laser pulses at an extremely high-pulse repetition frequency, typically near 100 MHz. The average power is typically several hundred milliwatts. This combines to produce approximately 10 nJ of energy per pulse. With such a large repetition frequency, exposed tissue reacts with the same damage mechanism to pure CW exposures. Although this thermal damage occurs at the same exposure level for CW and femtosecond oscillator laser exposures, some differences in pathological and cellular responses have been reported.¹²

The femtosecond amplifier illustrated in the bottom half of Figure 12-1 uses the output pulse train from a femtosecond oscillator. These pulses are first *stretched*, which means that the pulse duration is significantly lengthened. This is done because, as pulses are amplified, short femtosecond pulses would exceed the damage irradiance threshold for the mirrors and optics of the system. Stretched pulses allow the amplifier peak irradiances to remain below damage thresholds for internal optics. The amount of stretching necessary depends on input pulse characteristics, but any input pulse is typically stretched from one to several hundred picoseconds. A pulse selector is used to inject very few of the hundreds of millions of femtosecond pulses into the amplifier section of the laser system. A very high-energy pulsed pump laser intersects the Ti:Sapph crystal simultaneously with the injected femtosecond pulse. This pulsed pump laser runs at

the same rate as the injected pulses, typically at 10 to 1,000 Hz. As noted in Figure 12-1, the pump light (typically green for Ti:Sapph amplifiers) is injected into the system through one of the near-infrared laser amplifier “pump-through” mirrors. The resulting low-repetition rate pulses circulate in the amplifier cavity for several round trips until the pulse energy has been increased through successive passes through the Ti:Sapph crystal. When pulse energy is sufficiently high, the pulse is ejected from the amplifier section into the compressor. In the compressor, the pulse lengthening that was achieved by stretching is reversed. The pulse is compressed to a significantly shorter pulse. The eventual shortest pulse duration is limited by the input pulse bandwidth due to the bandwidth-limiting process discussed earlier in this chapter. Pulse energy is limited by the amount of available pump energy, and by the size and saturation of the Ti:Sapph crystal because of thermal loading from optical pumping.

As shown, femtosecond oscillators produce low-energy pulses at very high repetition frequencies, and femtosecond laser amplifiers produce high-energy pulses with extreme peak powers at relatively low-pulse repetition frequencies. The eventual output of the femtosecond amplifier is typically several millijoules of energy in approximately 100 fs pulses. This produces several gigawatts of peak power, making possible many nonlinear optical mechanisms. As will be discussed later, these same nonlinear mechanisms may occur in many laser–tissue interaction scenarios.

MEASUREMENT OF ULTRASHORT LASER PULSES

Because ultrashort lasers have special properties, special care must be taken to characterize femtosecond laser pulses that have

- extremely short pulse duration,
- large peak irradiances, and
- large bandwidths.

Some techniques of measurement apply equally well to femtosecond, nanosecond, and microsecond laser pulses. However, it is often the case that special techniques must be used to characterize femtosecond pulse duration.

Traditional Measurement Techniques

Pulse energy and wavelength measurements of femtosecond pulses can be taken in much the same way as longer wavelength pulses. The same energy

detectors that are used to measure typical Q-switched nanosecond pulse energy can also be used to measure femtosecond laser energy. Usually, this requires no change in setup or detector, although higher detector sensitivity may be required to adjust for the fact that typical femtosecond laser pulses have less energy than do their Q-switched counterparts. Laser wavelength can be measured easily thanks to the development of integrating spectrometer units (eg, those that fit on a PC [personal computer] board). A fiberoptic can be used to collect light and deliver it to the time-integrating spectrometer. The wavelength bandwidth will be greater for femtosecond laser pulses and, therefore, the resolution requirements are somewhat relaxed for measurement of laser bandwidth. The measurement of femtosecond pulse width is usually much more challenging, however. These challenges (the photodiode and oscilloscope and streak camera) are outlined in the next section.

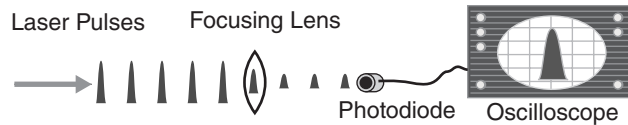


Figure 12-2. Typical setup for measuring pulse duration using an oscilloscope and photodiode.

Photodiode and Oscilloscope

The most commonly used method for measuring pulse duration is with a photosensitive element (eg, a photodiode) and an oscilloscope to detect its response. This method is illustrated in Figure 12-2. However, because the typical high-speed photodiode has a limiting rise time of 1 ns, this technique is not sufficient to precisely characterize a femtosecond laser pulse. The most carefully crafted photodiode with an extremely small detector surface coupled to a fiber achieves a 10 ps response time at best. Therefore, novel techniques have been devised to measure femtosecond laser pulse duration.

Streak Camera

A second method used for measuring laser pulses is a streak camera. A streak camera works in a manner similar to how a television tube electron gun diverts its beam. The streak camera first converts optical pulses into a package of electrons with similar duration and then sweeps the electrons with a pair of plates that diverts their position on a phosphorous screen. Unfortunately, this technique is also limited by minimum measurable pulse duration. The shortest pulse duration measurable by the streak camera is several hundred femtoseconds. The streak camera also requires a large capital investment on the order of several hundred thousand dollars.

Interferometric Measurements: Autocorrelation

Due to the limitations of traditional measurement techniques, more novel means have been devised to measure the pulse duration of femtosecond lasers. These techniques usually involve splitting a pulse and optically interfering the pulse on itself. The first such technique is the *second harmonic autocorrelator* (illustrated in Figure 12-3) that requires multiple pulses. A femtosecond laser pulse is split into two equivalent beams. These beams are then intersected in a frequency-doubling crystal. One of the beam

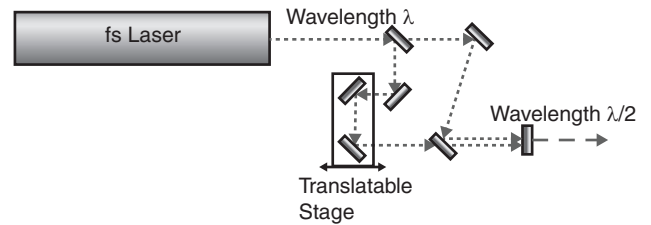


Figure 12-3. Measurement of femtosecond laser pulse using second harmonic autocorrelation.

fs: femtosecond

paths has a variable length that is swept from a longer path through an equivalent path to a shorter path. This produces increasing second harmonic generation radiation as a function of the multiplicative pulse energies. The result is a unique pattern in second harmonic intensity as a function of beam path difference.

The result of this measurement has been uniquely correlated with pulse duration. The output is a plot of second harmonic intensity versus the relative positions of the pulses (ie, time between peaks arriving at center of the crystal). This measurement correlates real-spatial coordinates with time, allowing for resolutions equivalent to several femtoseconds if the accuracy of the stage is on the order of several micrometers. This autocorrelation technique has been adapted for both low-repetition and high-repetition rate systems (eg, mode-locked lasers).

A number of other techniques have also been developed for pulse width measurement, primarily for lasers shorter than 50 fs. Examples include the following:

- frequency-resolved optical gating (FROG),
- spectral-phase interferometry for direct electric field reconstruction (SPIDER),
- temporal analysis by dispersing a pair of light E-fields (TADPOLE), and
- grating-eliminated no-nonsense observation of ultrafast incident laser light E-fields (GRENOUILLE).

These advanced measurement techniques are used to determine the relative phase of the laser pulse in addition to its pulse duration. The phase of an ultrashort pulse is the relationship between the differing spectral content in spatial position and extent. Phase is relevant for pulse durations shorter than 100 fs and for propagation of pulses in biologically significant distances.

ULTRASHORT LASER EFFECTS ON THE RETINA

Nanosecond to Femtosecond Minimum Visible Lesion Thresholds

The first scientific reports on injury to the retina from subnanosecond laser pulses were published^{13,14} in 1974 and 1975, using 25 to 35 ps pulses, and reported a threshold of $13 \pm 3 \mu\text{J}$ at 1,064 nm. Experiments during this period used rhesus monkey eyes in vivo as the model of choice to determine retinal injury thresholds. The injuries observed in these studies were recognized as different from retinal thermal injuries previously noted by researchers who employed longer duration exposures^{15,16} using the same model. It was speculated that the unusual retinal injuries may be due to nonlinear effects. Researchers theorized that melanin granules were responsible for retinal light absorption in a way that differed from simple thermal denaturation of retinal tissue. Immediate subretinal hemorrhages were reported at 150 μJ , and comparison to previous work showed a dramatic departure of threshold values using Nd:YAG Q-switched sources as seen in Table 12-2.

These experimental findings reinforced the hypothesis that the effects of subnanosecond pulses occurred by a mechanism other than thermal denaturation. Histological evaluation led many of the earlier investigators to speculate that retinal damage originated from photomechanical shock waves originating in melanin granules. They found that a change in radiant exposure was not linearly dependent on exposure beam diameter, as would be the case in a thermal damage model. Therefore, a new nonthermal mechanism for damage was found to be necessary for ultrashort laser exposures.

In 1978, Taboada and Gibbons¹⁷ applied probit analysis¹⁸ and reported an ED₅₀ (estimated dose for 50% probability of laser-induced damage) at 95% confidence

level as 2.2 μJ (fiducial limits: 1.9 and 2.5 μJ) at 24-h postexposure for 5.9 ps using a wavelength of 1,060 nm. Based on this work, the minimum visible lesion (MVL) criterion was defined as the smallest ophthalmoscopic-observable grayish opacification differing from the retinal background viewed by an observer at 1- and 24-h postlaser exposure. The investigators provided both 1- and 24-h ED₅₀s for 1,064 nm 5.9 ps pulses (3.5 and 2.2 μJ , respectively). At the time, these pulses were the shortest investigated in vivo, and the authors discussed possible nonlinear effects, such as the four-photon process, dielectric breakdown, and increases in short-wavelength radiation (superbroadening).

In 1982, Bruckner and Taboada¹⁹ reported on the effects of laser pulses of 6 ps in duration operating at 530 nm and delivered to the retina in vivo. The 24-hour ED₅₀ was again determined by probit analysis and found to be 0.24 μJ (0.17–0.35 μJ) corresponding to a retinal irradiance of $4.4 \times 10^{-3} \text{ J cm}^{-2}$, with a correction of 0.88 for ocular transmission and a spot size at the retina reported as 78 μm . When compared with earlier work by Goldman et al²⁰, who determined a threshold of 18.2 μJ with a retinal spot size of 25 μm , an irradiance of 6.5 J cm^{-2} for 30 ps is easily calculated. The results immediately suggest nonlinear effects scaling with pulse power (Bruckner and Taboada¹⁹ measured 0.73 GW cm^{-2} , and Goldman et al²⁰ measured 220 GW cm^{-2}). Bruckner and Taboada¹⁹ argued that the integrated irradiance of $4.4 \times 10^{-3} \text{ J cm}^{-2}$ at 6 ps could only create a small temperature rise, calculated as an increase of 4.0° C above ambient. Because this thermal rise would decay rapidly within microseconds, it would not be sufficient to cause phase change such as that typically associated with thermal retinal damage induced by longer duration laser exposures. This work sparked more than a decade of controversy concerning the validity of the data by Bruckner and Taboada.

The first femtosecond pulse retinal damage was reported in 1987 by Birngruber et al,²¹ who worked with the Chinchilla grey rabbit model. The ED₅₀s measured ophthalmoscopically and angiographically were reported as 4.45 μJ and 0.75 μJ , respectively. Visible lesions were created using a 632 nm laser with 80 fs single pulses delivered directly to the retina and a controlling external optic to achieve an 80- μm diameter spot consistently on the retina. Albino rabbits were also used to compare and consider the role of melanin. Interestingly, the albino rabbit retinas were not injured by the 80 fs pulses. In the Chinchilla grey rabbits, the type of damage observed at threshold energies appeared no different, even at pulse energies 100 times that of the ED₅₀. In fact, researchers were unable to produce a subretinal hemorrhage at any energy. This provided clear

TABLE 12-2

PRELIMINARY INDICATION OF DEPARTURE FROM THERMAL DAMAGE MECHANISMS WHEN SUBNANOSECOND LASER PULSES ARE USED TO DETERMINE RETINAL THRESHOLDS

Pulse Duration	Retinal Threshold (μJ)	Wavelength (nm)	Reference
30 ns	280	1,064	15
15 ns	68 ± 12	1,064	13
10 ns	164	1,064	16
30 ps	8.7 ± 4.8	1,064	17
30 ps	18.2 ± 8.3	532	17

Data sources: see References

experimental evidence that the injuries caused by 80 fs pulses were due to nonlinear rather than thermal effects. Investigators also noted that melanin was central to the mechanism of retinal damage even at femtosecond laser exposures. Nonlinear mechanisms appeared to be a reasonable explanation as to why the extent of retinal damage was limited at energies well above threshold.

In 1995, Cain et al²² reported the first comprehensive subnanosecond retinal damage study using rhesus monkeys (Table 12-3). They were able to compare their data to previous work and found that Bruckner and Taboada's data fit within the experimental error of their own. This brought an end to the long controversy. But with the new data came new questions concerning the departure from a thermal damage model, the absence of a trend in the data as a function of wavelength,²³ and issues surrounding the role of nonlinear phenomena, such as thermal acoustic transients, LIB, self-focusing, and continuum generation.

Damage Mechanisms

As questions persisted concerning the basis of retinal damage from subnanosecond laser pulses, simultaneous work in the 1980s and 1990s found scientists exploring the impact of nonlinear laser-induced phenomena on the human eye.²⁴ In particular, it was interesting that such nonlinear phenomena might be put to use as ophthalmological treatments for eye diseases.²⁵⁻³⁵ Of particular interest were the nonlinear phenomena of

- self-focusing,
- stimulated Brillouin scattering (SBS),
- supercontinuum generation, and
- laser-induced breakdown.

These phenomena had been well characterized experimentally and theoretically for homogeneous nonbiological materials. Their potential influence on the human retina would yet have to be considered in terms of laser beam spot size, wavelength, and pulse duration. These are the characteristics essential to determining the resultant peak power (critical power) at which phenomena of interest become viable as a pulse of laser light makes its way from the cornea to the retina.³⁶

Self-Focusing

Self-focusing is an induced lensing effect that results from wavefront distortion inflicted on the beam by itself. Consider a laser beam with a Gaussian profile propagating into a medium with a refractive index, n , given by

TABLE 12-3

MINIMUM VISIBLE LESION THRESHOLD AT THE 95% CONFIDENCE LEVEL (SHOWN IN PARENTHESES)

Pulse Duration	ED ₅₀ (μJ) @24 Hours	Wavelength (nm)	Reference
4 ns	0.9 (0.60–1.35)	532	22
80 ps	4.2 (3.0–5.8)	1,064	23
60 ps	0.43 (0.32–0.54)	532	22
20 ps	4.6 (3.8–5.5)	1,064	23
6 ps	0.24 (0.17–0.35)	530	20
3 ps	0.58 (0.31–0.83)	580	22
1 ps	2.0 (1.4–2.5)	1,060	23
600 fs	0.26 (0.21–0.31)	580	22
150 fs	1.0 (0.8–1.2)	1,060	23
100 fs	0.16 (0.11–0.23)	530	23
90 fs	0.43 (0.27–0.60)	580	22
44 fs	0.17 (0.13–0.22)	810	24

Data sources: see References

$$n = n_0 + \Delta n(|E^2|) \sim n_0 + n_2 |E^2|,$$

where

n_0 = the linear refractive index of the medium,
 n_2 = the nonlinear refractive index of the medium,
 E = the electric field of the laser pulse, and
 $|E^2|$ = directly proportional to the power of the laser pulse.

If $\Delta n(|E^2|)$ is positive and the beam has achieved a critical power sufficient to overcome n_0 , then the central part of the beam (having a higher intensity) will experience a larger refractive index than the beam edge. The central part of the beam will undergo a distortion similar to that imposed on the beam by a positive lens. Thus, it will appear to focus by itself. Self-focusing leads to an increase in irradiance, which can in turn contribute to other nonlinear optical effects. Two self-focusing effects have been described in detail^{37,38} as having potential impact on subnanosecond retinal damage. Weak self-focusing has a threshold of occurrence below 10 ps. Critical beam collapse has a threshold below 100 fs when compared to MVL data. Note that the critical power for beam collapse in water has been reported as near 500 kW peak power.³⁸

Stimulated Brillouin Scattering

SBS is laser light scattering from refractive index variations associated with sound waves generated in a medium by a laser pulse. The most common mechanism

for the creation of such sound waves is *electrostriction*, where there is a tendency of the medium to become compressed in an area of high intensity. In general, when the thresholds for SBS are compared to MVL data from the visible spectrum, the conclusion is that SBS would not be a factor in the resultant retinal damage for visible wavelengths. Further, if one considered near-infrared pulses around 1,064 nm with a pulse duration of 1 ns and a damage threshold of 1 mJ cm⁻², a critical power of 385 kW could be achieved within the threshold for SBS. However, this would lead to an increase in the retinal damage threshold because a percentage of the laser light would be backscattered away from the retina.

Supercontinuum Generation

Supercontinuum generation occurs when a pulse of laser light reaches a critical power within a medium and the nonlinear refractive index changes during propagation, thus leading to the production of a wide spectral bandwidth. When required critical peak power is compared to MVL data below 1 ns, the conclusion is that supercontinuum generation is not a contributing factor to subnanosecond MVLs in the visible spectral region. In general, when compared to actual retinal threshold data, the regime in which supercontinuum generation is calculated to change the characteristics of the forward propagating beam is near 1 fs. With the multiphoton excitation increases in the 2014 release of the ANSI (American National Standards Institute) Z136.1³⁹ standard (*Safe Use of Lasers*) for the 1.2 to 1.4 μm range, the possibility of supercontinuum generation needs to be evaluated where incident peak powers at the cornea approach the critical power for self-focusing after propagation with absorption into the eye. Further research is warranted.

Laser-Induced Breakdown

LIB offers the most plausible explanation for observed anomalies in the trends away from thermal-induced lesions above the 1 ns exposure time domain. LIB is a catastrophic dielectric breakdown due to extremely large electric fields associated with high peak powers when laser pulses are focused into a medium (solid, liquid, or gas). This effect can be coupled with self-focusing. Dielectric breakdown through optical absorption of laser radiation is the partial or complete ionization of the medium. This ionization results in a gas of charged particles called *plasma*, which absorbs optical radiation much more strongly than ordinary matter. Associated with the plasma is rapid heating by the laser pulse, expansion of the plasma, an audible acoustic signature, and a visible emission.

LIB may occur from either of two distinct mechanisms: (1) *indirect ionization* (avalanche ionization) of the medium and (2) *direct ionization* (multiphoton absorption) of the medium. By using indirect ionization, one or more “free” electrons must be in the focal volume of the pulse to initiate the process whereby free or “seed” electrons can absorb light through collisions with atoms or molecules. Avalanche ionization occurs when an energy greater than the ionization potential is reached by a free electron, which in turn transfers energy through collision with another atom or molecule to produce a second free electron, and the process continues geometrically until breakdown is achieved. With direct ionization, each electron is independently ionized, thus requiring no free electrons or collision processes to drive it. Multiphoton ionization is a process that becomes significant only at high irradiances and wavelengths in the near-infrared or shorter regime.

To consider LIB in terms of MVL production in the eye, the mechanisms described previously require an understanding of focused beam wavelength, pulse duration, and spot size that lead to the critical power needed for the event to occur. Kennedy⁴⁰ identifies three laser pulse exposure time domains of concern:

1. a long pulse regime (>100 ns) dominated by avalanche ionization;
2. a short pulse regime (100 ns–200 fs), where both types of ionization can be significant; and
3. an ultrashort pulse regime (<200 fs) dominated by multiphoton ionization.

In the 100 ns to 200 fs time domain, the laser pulse may be so short that avalanche ionization cannot occur unless a multiphoton ionization process “jump starts” the avalanche process. Note that below the thresholds necessary for the previously described processes, a fourth process can occur that is initiated by any one of the three processes. Specifically, very hot gas bubbles can form in the focal region of the laser pulse. This process does not quite reach a full-blown LIB as described by the formation of a visible event or acoustic signature.^{41,42}

Table 12-4 summarizes our laboratory’s predicted nonlinear threshold phenomena as it compares to experimental ED₅₀ thresholds at 24 hours postretinal exposure. Here, the two LIB processes (avalanche and multiphoton ionization) are not comparable with the much lower ED₅₀ thresholds down to 90 fs. However, the self-focusing threshold does become comparable between 600 fs and 90 fs, respectively. In fact, there is an increase in the avalanche threshold from 600 fs to

TABLE 12-4

THRESHOLD ENERGIES FOR SEVERAL NONLINEAR PHENOMENA COMPARED TO THE RETINAL DAMAGE THRESHOLD

Pulse Duration	ED ₅₀ at 24 Hours (μJ)	Retinal Image Diameter (μm)	Self-Focusing Threshold (μJ)	Avalanche Threshold (μJ)	Multiphoton Threshold (μJ)
4 ns: 532 nm	0.9	30	2,400	181.0	9,536
60 ps: 532 nm	0.43	39	36	33.6	580
6 ps: 530 nm	0.24	39	3.6	13.6	99
3 ps: 580 nm	0.58	30	2.1	15.4	156
600 fs: 580 nm	0.26	30	0.43	13.3	83
90 fs: 580 nm	0.43	30	0.06	32.7	20

90 fs, respectively, whereas the multiphoton threshold process continues to diminish.

Studies are currently underway to determine the response of the retina to exposure to laser pulses

shorter than 100 fs. Current laser safety standards do not provide maximum permissible exposure levels for these shortest pulses. Cain et al⁴³ showed that retinal threshold damage for exposures <90 fs is the result of

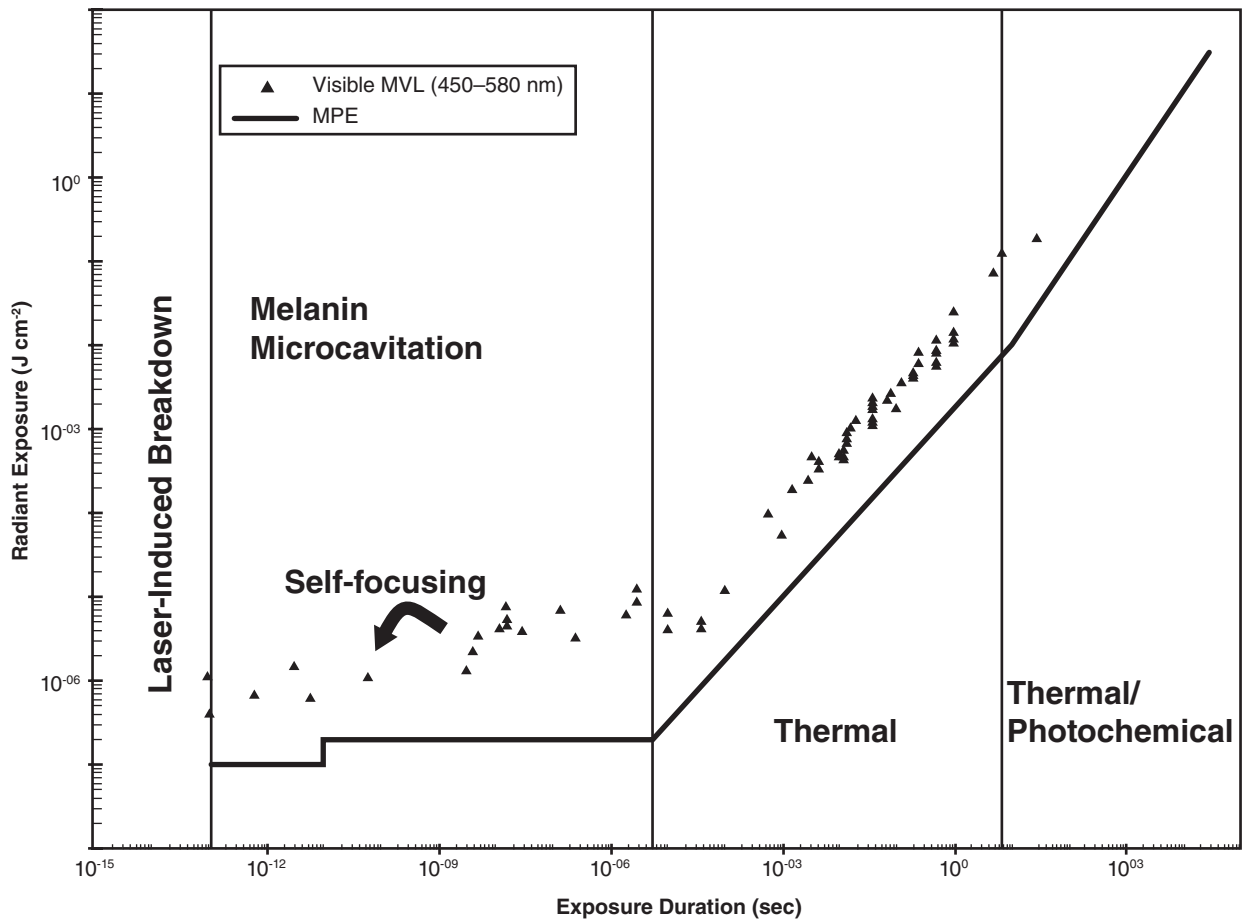


Figure 12-4. Damage mechanisms are listed as labels on this plot of single-pulse laser exposure threshold versus duration (data points). The lines are the current maximum permissible exposure levels from the ANSI Z136-2014 standard. MPE: maximum permissible exposure; MVL: minimal visible lesion

LIB in the retina. Another study by Cain et al²⁴ reported the retinal damage threshold for a 40 fs laser exposure, which is the shortest-duration laser pulse to create a retinal lesion ever recorded. Also, the damage energies for retinal lesions described in that report were made with the smallest single-pulse energy (0.17 μJ) of any study ever published. The authors found that, depending on how the pulse was preconditioned, retinal damage threshold could be reduced from 0.25 μJ per pulse to 0.17 μJ per pulse, respectively. Beam preconditioning was achieved by adjusting the phase of the pulse, which is the relative position in time of the longer wavelength portion to the shorter wavelength portion. This effect was shown to be more pronounced as pulse duration decreased below 20 to 50 fs for wavelengths of 450 to 800 nm, respectively (see Table 12-1). The effects on propagation for these shortest pulse durations are defined by GVD (Figure 12-4). It is believed that the modeling done by Cain et al²⁴ can be extended to determine the expected retinal

damage thresholds for all retinal hazard wavelengths for pulse durations below 100 fs. If so, this will allow future safety standards to establish maximum permissible exposure levels for sub-100 fs laser exposures. Figure 12-4 summarizes our discussion on retinal damage mechanisms.

Thermal and photochemical damage are delineated in Figure 12-4 for pulses longer than approximately 20 μs . These are long-term exposures whereby heat can produce protein denaturation or photochemical damage can occur for long-term, blue-to-green exposures. For pulse durations between 100 fs and 20 μs , respectively, Lin et al⁴⁴ have shown that microcavitation around melanosomes of the retina can induce cell injury. This is delineated in Figure 12-4 as melanin microcavitation. For pulse durations on the order of 1 ps, Rockwell et al³⁶ have shown that self-focusing can occur, thus reducing the retinal spot size and thereby reducing the corneal irradiance required for minimal damage.

ULTRASHORT LASER EFFECTS ON THE SKIN

There have been three studies documenting damage to the skin from femtosecond exposures.⁴⁵⁻⁴⁷ These studies result in different conclusions, possibly because their parameters are slightly different. Watanabe et al⁴⁵ used an amplified 65 fs laser pulse at 630 nm to study the damage threshold for producing immediate whitening (and ultrastructural changes in melanosomes) utilizing the black guinea pig skin model. Using a 50 μm spot size, they found that, at 0.31 J cm^{-2} , there was melanosome disruption. No other damage was seen up to 0.58 J cm^{-2} . At 0.92 J cm^{-2} , the investigators noted increased electron density of the cytoplasm in electron microscopy of the area. They further observed that when gross and ultrastructural damage thresholds of melanin were plotted versus pulse width, there was a near-constant fluence damage threshold for 65 fs to 10 ns, and an increase in threshold for 40 ns to 0.4 ms exposure durations.

Frederickson et al⁴⁶ employed 800 nm, 120 fs laser exposures using 1 mm spot size exposures to measure the ablation threshold for skin. They used shaved, Sprague-Dawley female rats as their skin model. The threshold energy for tissue ablation was 2 mJ, which translates to 2.5 TW cm^{-2} peak power or a radiant exposure of 0.26 J cm^{-2} . Very little tissue was removed

with these threshold exposures because it took 100 pulses to ablate the epidermis.⁴⁶ Using 9 mJ per pulse, 10 pulses would remove the epidermis.

Kumru et al⁴⁷ used 810 nm, 44 fs laser exposures with sufficient propagation distance to allow the beam to collapse to a filament (or set of filaments) before impinging the skin of Yucatan mini-pigs. Using this setup, they determined that a pulse energy of 8.2 mJ produced a minimally visible ED_{50} lesion 1 hour after exposure. This damage threshold corresponds to the energy required to produce a femtosecond filament, implying that this phenomenon was required for these low-pulse energies to produce skin damage.

Examination of these three studies highlights the importance of relative biophysical thresholds in determining the damage from lasers. The ablation threshold for femtosecond laser exposure is near the threshold for melanosome disruption; but, if the peak power in the beam is sufficient for a filament to be created, a lower threshold for skin damage may be possible. Both of these phenomena will lead to skin damage, but the threshold for damage will depend on which phenomenon leads to a lower threshold for any given combination of pulse width, wavelength, propagation distance, and spot size.

ULTRAFAST, ULTRAINTENSE LASERS

It is necessary to consider the effects produced by ionizing radiation as a byproduct and therefore a safety challenge for femtosecond lasers operating at ultra-

intense power densities. Technological advances have led to the development of lasers with extreme powers and intensities, where the current record set by the

HERCULES laser in 2008 achieved a focal intensity of $2 \times 10^{22} \text{ W cm}^{-2}$.⁴⁸ This was achieved at the University of Michigan in 2008 through the use of adaptive optics that provided an ideal focusing of the laser pulse, thus achieving a peak power of 300 TW. Several facilities in the world can now provide laser pulses of 1 PW (where TW is the terawatt unit or 10^{12} W and PW is petawatt unit or 10^{15} W).

Intensities on the order of $10^{12} \text{ W cm}^{-2}$ correspond to field strengths that are capable of perturbing electrons at the highest energy levels strong enough to cause a nonlinear response. At intensities of the order of $10^{14} \text{ W cm}^{-2}$, laser fields start to compete with intraatomic fields, causing rapid ionization and complex dynamics of electrons. As available laser intensity has reached a level of the order of $10^{16} \text{ W cm}^{-2}$, laser fields begin to surpass the intraatomic fields that bind electrons, thus providing the mechanism for rapid ionization of various targets and for studies considering nonlinear processes. Between 10^{16} and $10^{22} \text{ W cm}^{-2}$, competing matter interaction

mechanisms are operative that account for the induced relativistic motion of electrons, relativistic self-induced transparency, and the ability to overcome the ponderomotive force that is responsible for excitation of Langmuir waves by a laser pulse propagating in undersense media.^{49,50}

It is important to consider the interaction of ultrashort, ultraintense laser light with matter where ionizing radiation may be produced in terms of the potential hazard and how in the process this hazard can be mitigated. In one such reported study, Qiu et al⁵¹ note that a very limited number of studies have considered the issue of laser-induced ionizing radiation protection. In their work, they focused on the physics and characteristics of laser-induced X-ray hazards. Their concern centered on the possible X-ray dose rate associated with 4 TW and a peak intensity of $2.4 \times 10^{18} \text{ W cm}^{-2}$. Their conclusion called for a graded approach to mitigate the laser-induced X-ray hazard with a combination of engineered and administrative controls being proposed.

SUMMARY

Femtosecond lasers are finding application in a host of novel applications. Here, we have described the novel damage that is seen with femtosecond laser exposure to the retina and skin. Femtosecond laser pulses create tissue damage with the reduction of photoacoustic effects, resulting in more precise damage zones.^{3,52,53} With damage mechanisms found to occur, treatment and injury response are possible. Multipho-

ton absorption in microscopy and DNA dissection techniques have made possible several new fields of study related to the use of femtosecond laser pulses with no photomechanical effect. Although battlefield applications may be years away, ultrashort lasers will inevitably be militarized, and their eventual utility will likely be determined by their initial application in nonmilitary settings.

REFERENCES

1. Juhasz T, Djotyan G, Loesel FH, et al. Applications of femtosecond lasers in corneal surgery. *Laser Phys.* 2000;10:1–6.
2. Schutze K, Poesl H, Lahr G. Laser micromanipulation systems as universal tools in molecular biology and medicine. *Cell Mol Biol.* 1998;44:735–746.
3. Tirlapur UK, Konig K, Peuckert C, Krieg R, Halbhuber KJ. Femtosecond near-infrared laser pulses elicit generation of reactive oxygen species in mammalian cells leading to apoptosis-like death. *Exp Cell Res.* 2001;263:8–97.
4. Konig K, Riemann I, Fischer P, Halbhuber K. Intracellular nanosurgery with near infrared femtosecond laser pulses. *Cell Mol Biol.* 1999;45:195–201.
5. Konig K, Riemann I, Fritsche W. Nanodissection of human chromosomes with near-infrared femtosecond laser pulses. *Opt Lett.* 2001;26(8):19–82.
6. Venugopalan V, Guerra A, Nahen K, Vogel A. The role of laser-induced plasma formation in pulsed cellular microsurgery and micromanipulation. *Phys Rev Lett.* 2002;88(7):1–4.
7. Minoshima K, Kowalevicz AM, Hartl I, Ippen E, Fujimoto JG. Photonic device fabrication in glass by use of nonlinear materials processing with a femtosecond laser oscillator. *Opt Lett.* 2001;26:1516–1518.

8. Schaffer B, Brodeur A, Garcia JF, Mazur E. Micromachining bulk glass by use of femtosecond laser pulses with nano-joule energy. *Opt Lett*. 2001;26:93–95.
9. Beier HT, Noojin GD, Rockwell BA. Localized thermal mapping using coherent anti-Stokes Raman spectroscopy. *J Biomed Opt*. 2012;17(8):0805011–0805013.
10. Hammer DX, Welch AJ, Noojin GD, Thomas RJ, Stolarski DJ, Rockwell BA. Spectrally resolved white-light interferometry for measurement of ocular dispersion. *J Opt Soc Am A*. 1999;16(9):2092–2102.
11. Alfano RR. *The Supercontinuum Laser Source*. New York, NY: Springer-Verlag; 1989.
12. Thomas RJ, Noojin GD, Stolarski DJ, et al. A comparative study of retinal effects from continuous wave and femtosecond mode-locked lasers. *Lasers Surg Med*. 2002;31(1):9–17.
13. Ham WT, Mueller HA, Goldman AJ, Newman BE, Holland LM, Kuwabara T. Ocular hazard from picosecond pulses of Nd:YAG laser radiation. *Science*. 1974;185:362–363.
14. Goldman AI, Ham WT, Mueller HA. Mechanisms of retinal damage resulting from the exposure of rhesus monkeys to ultrashort laser pulses. *Exp Eye Res*. 1975;21:457–469.
15. Vassiliadis A. Thresholds of laser eye hazards. *Arch Environ Health*. 1970;20:161–170.
16. Ebbers RW, Dunskey IL. Retinal damage thresholds for multiple-pulse lasers. *J Aerospace Med*. 1973;44:317–318.
17. Taboada J, Gibbons WD. Retinal tissue damage induced by single ultrashort 1060 nm laser light pulses. *Appl Opt*. 1978;17:2871–2873.
18. Finney DJ. *Probit Analysis*. 3rd ed. New York, NY: Cambridge University Press; 1971.
19. Bruckner A, Taboada J. Retinal tissue damage induced by 6-psec 530-nm laser light pulses. *Appl Opt*. 1982;31(3):365–367.
20. Goldman AI, Ham WT, Mueller HA. Ocular damage thresholds and mechanisms for ultrashort pulses of both visible and infrared laser radiation in the rhesus monkey. *Exp Eye Res*. 1977;24:45.
21. Birngruber R, Puliafito CA, Gawande A, Lin WZ, Schoenlein RT, Fujimoto JG. Femtosecond laser-tissue interactions: retinal injury studies. *IEEE J Quantum Electron*. 1987;QE-23(10):1836–1844.
22. Cain CP, Toth CM, DiCarlo CA, et al. Visible retinal lesions from ultrashort laser pulses in the primate eye. *Invest Ophthalmol Vis Sci*. 1995;36(5):879–888.
23. Cain CP, Toth CA, Noojin GD, Carothers V, Stolarski DJ, Rockwell BA. Thresholds for visible lesions in the primate eye produced by ultrashort near-infrared laser pulses. *Invest Ophthalmol Vis Sci*. 1999;40:2343–2349.
24. Cain CP, Thomas RJ, Noojin GD, et al. Sub-50-fs laser retinal damage thresholds in primate eyes with group velocity dispersion, self-focusing and low-density plasmas. *Graefe's Arch Clin Exp Ophthalmol*. 2005;243(2):101–112.
25. Boppart SA, Toth CA, Roach WP, Rockwell BA. Shielding effectiveness of femtosecond laser-induced plasmas in ultrapure water. *Proc SPIE*. 1993;1882:347–354.
26. Capon M, Mellerio J. Nd:YAG lasers: plasma characteristics and damage mechanisms. *Lasers Ophthalmol*. 1986;1(2):95–105.
27. Docchio F, Dossi L, Sacchi CA. Q-switched Nd:YAG laser irradiation of the eye and related phenomena: an experimental study. III. Experimental observation of stimulated Brillouin scattering in eye models. *Lasers Life Sci*. 1986;1(2):117–124.
28. Docchio F, Sacchi A. Shielding properties of laser-induced plasmas in ocular media irradiated by single Nd:YAG pulses of different durations. *Invest Ophthalmol Vis Sci*. 1988;29(3):437–443.

29. Powell JA, Moloney JV, Newell AC, Albanese RA. Beam collapse as an explanation for anomalous ocular damage. *J Opt Soc Am B*. 1993;10(7):1230–1241.
30. Rockwell BA, Roach WP, Rogers M, et al. The nonlinear optical properties of ocular components. *Opt Lett*. 1993;18(21):1792–1794.
31. Rockwell BA, Roach WP, Rogers ME. Determination of self-focusing effects of light propagating in the eye. *Proc SPIE*. 1994;134A:2–9.
32. Sacchi CA. Laser-induced electric breakdown in water. *J Opt Soc Am B*. 1991;8(2):337–345.
33. Sheik-Bahae M, Said AA, Wei TH, Hagan DJ, Stryland EV. Sensitive measurement of optical nonlinearities using a single beam. *IEEE J Quantum Electron*. 1990;QE-26(4):760–769.
34. Steinert RF, Puliafito CA, Trokel S. *Am J Ophthalmol*. 1983;96:427.
35. Zysset B, Fujimoto JG, Deutsch TF. Time-resolved measurements of picosecond optical breakdown. *Appl Phys B*. 1989;48:139–147.
36. Rockwell BA, Thomas RJ, Vogel A. Ultrashort laser pulse retinal damage mechanisms and their impact on thresholds. *Med Laser Appl*. 2010;25(2):84–92.
37. Rockwell BA, Kennedy PK, Thomas RJ, Roach WP, Rogers ME. The effect of nonlinear optical phenomena on retinal damage. *Proc SPIE*. 1995;2391:89–95.
38. Smith WL, Liu P, Bloembergen N. Superbroadening in H₂O and D₂O by self-focused picosecond pulses from a YAlG:Nd laser. *Phys Rev A*. 1977;16(6):2396–2404.
39. American National Standards Institute. *The Safe Use of Lasers*. ANSI Z136.1–2014. Orlando, FL: Laser Institute of America; 2014.
40. Kennedy PK. A first-order model for computation of laser-induced breakdown thresholds in ocular and aqueous media. Part I. Theory. *IEEE J Quantum Electron*. 1995;QE-31:2241.
41. Vogel A, Busch S, Parlitz U. Shock wave emission and cavitation bubble generation by picosecond and nanosecond optical breakdown in water. *J Acoust Soc Am*. 1996;100:148–165.
42. Vogel A, Noack J, Nahen K, et al. Energy balance of optical breakdown in water at nanosecond to femtosecond time scales. *Appl Phys B*. 1999;68:271–280.
43. Cain CP, DiCarlo CD, Rockwell BA, et al. Retinal damage and laser-induced breakdown produced by ultrashort pulse lasers. *Graefes Arch Clin Exp Ophthalmol*. 1996;234(suppl 1):S28.
44. Lin C, Kelly M, Sibayan S, Latina M, Anderson R. Selective cell killing by microparticle absorption of pulsed laser radiation. *IEEE Select Top Quantum Electronics*. 1999;5(4):963–968.
45. Watanabe S, Anderson R, Brorson S, Dalickas G, Fujimoto J, Flotte T. Comparative studies of femtosecond to microsecond laser pulses on selective pigmented cell injury in skin. *Photochem Photobiol*. 1991;53(6):757–762.
46. Frederickson K, White W, Wheeland R, Slaughter D. Precise ablation of skin with reduced collateral damage using the femtosecond-pulsed, terawatt titanium-sapphire laser. *Arch Dermatol*. 1993;129:989–993.
47. Kumru SS, Cain CP, Noojin GD, et al. ED50 study of femtosecond terawatt laser pulses on porcine skin. *Lasers Surg Med*. 2005;37:59–63.
48. Yanovsky V, Chvykov V, Kalinchenko G, et al. Ultra-high intensity-300-TW laser at 0.1 Hz repetition rate. *Opt. Express*. 2008;16:2109–2114.

49. Farina D, Bulanov SV. Relativistic electromagnetic solitons in the electron-ion plasma. *Phys Rev Lett.* 2001;86(23):5289–5292.
50. Fedotov AM, Narozhny NB, Mourou G, Korn G. Limitations on the attainable intensity of high power lasers. *Phys Rev Lett.* 2010;105(8):080402.
51. Qiu R, Liu JC, Prinz AA, Rokni SH, Woods M, Xia Z. Analysis and mitigation of x-ray hazard generated from high intensity laser-target interactions. *ILSC Conf Proc.* 2011;127–135.
52. Noack J. Influence of pulse duration on mechanical effects after laser induced breakdown in water. *J Appl Phys.* 1998;83:7488–7495.
53. Vogel A. *Optical Breakdown in Water and Ocular Media and Its Use for Intraocular Photodisruption.* Lubeck, Germany: Lubeck Medical University, Medical Laser Center; 2000.